Skin electroporation of a plasmid encoding hCAP-18/LL-37 host defense peptide promotes wound healing

Skin Electroporation of a Plasmid Encoding hCAP-18/LL-37 Host Defense Peptide Promotes Wound Healing

Lars Steinstraesser[1], Martin C Lam[2,3], Frank Jacobsen[2], Paolo E Porporato[4], Kiran Kumar Chereddy[3], Mustafa Becerikli[2], Ingo Stricker[5], Robert EW Hancock[6], Marcus Lehnhardt[2], Pierre Sonveaux[4], Véronique Préat[3] and Gaëlle Vandermeulen[3]

[1]Department of Plastic, Reconstructive and Aesthetic Surgery, Handsurgery, Evangelisches Krankenhaus Oldenburg, European Medical School, Oldenburg, Germany;[2]Department of Plastic Surgery, Burn Center, BG University Hospital Bergmannsheil, Ruhr University Bochum, Bochum, Germany; [3]Louvain Drug Research Institute, Pharmaceutics and Drug Delivery, Université catholique de Louvain, Brussels, Belgium; [4]Institut de Recherches Experimentales et Cliniques, Pole of Pharmacology, Université catholique de Louvain, Brussels, Belgium; [5]Institute of Pathology, BG University Hospital Bergmannsheil, Ruhr University Bochum, Bochum, Germany; [6]Department of Microbiology and Immunology, University of British Columbia, Vancouver, British Columbia, Canada

Host defense peptides, in particular LL-37, are emerging as potential therapeutics for promoting wound healing and inhibiting bacterial growth. However, effective delivery of the LL-37 peptide remains limiting. We hypothesized that skin-targeted electroporation of a plasmid encoding hCAP-18/LL-37 would promote the healing of wounds. The plasmid was efficiently delivered to full-thickness skin wounds by electroporation and it induced expression of LL-37 in the epithelium. It significantly accelerated reepithelialization of nondiabetic and diabetic wounds and caused a significant VEGFa and interleukin (IL)-6 induction. IL-6 was involved in LL-37–mediated keratinocyte migration *in vitro* and IL-6 neutralizing antibodies delivered to mice were able to suppress the wound healing activity of the hCAP-18/LL-37 plasmid. In a hindlimb ischemia model, electroporation of the hCAP-18/LL-37 plasmid increased blood perfusion, reduced muscular atrophy, and upregulated the angiogenic chemokines VEGFa and SDF-1a, and their receptors VEGF-R and CXCR-4. These findings demonstrate that a localized gene therapy with LL-37 is a promising approach for the treatment of wounds.

Received 8 May 2013; accepted 16 October 2013; advance online publication 7 January 2014. doi:10.1038/mt.2013.258

INTRODUCTION

The treatment of difficult to heal wounds is a major clinical problem worldwide. In particular, chronic nonhealing skin ulcers are one of the major complications for diabetic patients. Skin and soft tissue infections are the most common indications for antimicrobial therapy[1] but the emergence of bacterial resistances against clinically used antibiotics complicates the treatment and underscores the need for new therapeutic options.[2,3] Antimicrobial peptides, also called host defense peptides, are effector molecules of innate immunity known to play a major role in nonspecific host defense against pathogens. They serve as first line of defense and display both direct killing of microbes and immunomodulatory properties.[4] The only antimicrobial peptide of the cathelicidin family identified in humans is hCAP-18/LL-37 and is produced as a prepropeptide. The extracellular cleavage of hCAP-18 by proteinase 3 releases a cathelin-like domain and the 37-amino-acid-long C-terminus LL-37 bioactive peptide.[5] In addition to its broad range of antimicrobial activities against bacteria, fungi, and viruses, human LL-37 appears particularly interesting for wound healing because it also promotes neovascularization.[6,7] Moreover, it is involved in reepithelialization and granulation tissue formation for skin wound repair.[8] Previous studies with mice deficient for the murine cathelicidin CRAMP, an ortholog of human LL-37, also uncovered a direct role in the maintenance of a first line of defense against bacterial skin infections.[9] In accordance with these findings, chronic wounds of elderly patients who fail to express LL-37 in the epidermis but still express LL-37 in polymorphonuclear neutrophils were colonized with *S. aureus*.[10] Recent clinical data about the expression of host defense peptides in diabetic foot ulcers revealed significant underexpression of LL-37 compared to healthy donors,[11] raising the hypothesis that a restoration of LL-37 expression might contribute to the healing of diabetes wounds.

The *in vivo* delivery of LL-37 is challenging. Indeed, topical wound treatment using LL-37 peptide was not able to promote healing in diabetic mice,[12] suggesting that proteolytic enzymes in diabetic wounds might have reduced the peptide half-life. It has been recently demonstrated that release of elastase by *P. aeruginosa* in chronic human ulcers inactivates LL-37 and induces hCAP-18 propeptide degradation in neutrophils, providing protection of bacteria against host defense mechanisms.[13] The human cathelicidin hCAP-18/LL-37 has previously demonstrated its potential to promote diabetic wound healing *in vivo* after cutaneous adenoviral gene delivery.[14] Adenoviral delivery of hCAP-18/LL-37 in *P. aeruginosa*-infected burn wounds led to high inhibition of

The first two authors contributed equally to this work.

Correspondence: *Véronique Préat, Université catholique de Louvain, Louvain Drug Research Institute, Avenue Mounier 73, bte B1.73.12, 1200 Brussels, Belgium. E-mail: veronique.preat@uclouvain.be*

bacterial growth, which was 1,000-fold stronger than with treatment by the synthetic LL-37 peptide,[15] suggesting a need for the sustained presence and continuous production of the peptide into the wound site. As viral gene transfer requires particular biosafety measures,[16] the development of nonviral delivery methods is appealing for potential clinical uses.[17,18] Another potential approach to deliver the gene of interest into wounds is the transplantation of *in vitro* transfected cells. Transplantations of virally transfected keratinocytes,[19] nonvirally transfected fibroblasts,[20] and adipose-derived stromal cells[21] are promising approaches for wound treatment. Although nonviral overexpression of hCAP-18/LL-37 in implanted skin tissues has shown promising activity *in vivo*,[22] direct nonviral techniques to deliver the transgene of interest would be more adequate for clinical use.

In this study, we hypothesize that the *in vivo* electroporation of a plasmid encoding hCAP-18/LL-37 would represent an efficient nonviral technique to overexpress LL-37 host defense peptide within wounds. *In vivo* DNA electroporation is one of the most powerful nonviral delivery methods promoting both permeabilization of cell membranes and electrophoresis of the injected DNA.[23] The combination of these two effects resulted in an enhanced transgene expression. Optimization of DNA electroporation into the skin led to a 100-fold increase in luciferase that was transiently expressed.[24,25] Electroporation of DNA encoding TGF-β,[26] KGF-1,[27] and HIF-1α[28] has previously been demonstrated to promote wound healing in leptin receptor-deficient db/db-mice. The study aimed at evaluating whether skin-targeted electroporation of a plasmid encoding hCAP-18/LL-37 would promote wound healing in nondiabetic and diabetic mice. In addition, the effect of this treatment was studied in a hindlimb ischemia model.

RESULTS

Combination of high- and low-voltage pulses allowed the most efficient gene expression into wounds

First, *in vivo* DNA electroporation in wounds was optimized by using reporter gene constructs to localize and quantify expression. After intradermal injection of a total amount of 50 µg of a plasmid encoding luciferase into four sites around each wound, we compared various electroporation parameters, as previously utilized for wound healing studies.[27,28] The combination of one 100 µs short, 700 V/cm high-voltage pulse immediately followed by one 400 ms long, 200 V/cm low-voltage pulse (HV+LV) induced a ~100-fold increase in luciferase expression in wounds 2 days after electroporation as compared to the injection of the plasmid without electroporation (no EP) ($P < 0.001$, analysis of variance (ANOVA)). The application of ten 20 ms 400 V/cm low-voltage pulses with 125 µs pauses between each pulse (LV) resulted in a lower but significant increase ($P < 0.01$), while six 100 µs short and 1,800 V/cm high-voltage pulses interspersed with 125 µs pauses were not able to significantly enhance luciferase expression compared to the no EP control, when applied using a plate-electrode (**Figure 1a**). Compared to LV or HV pulses alone, only the combination of HV+LV pulses displayed a significant increase in luciferase expression (approximately tenfold) on day 6 after electroporation ($P < 0.05$, ANOVA) (**Figure 1a**). The influence of the plasmid dose on luciferase expression was studied and 50 µg was found to be the optimal dose of plasmid ($P < 0.001$, ANOVA). A higher dose of DNA did not lead to a higher luciferase expression (**Figure 1b**). Examining the kinetics of luciferase production, the application of the HV+LV treatment led to significantly enhanced protein expression that peaked at

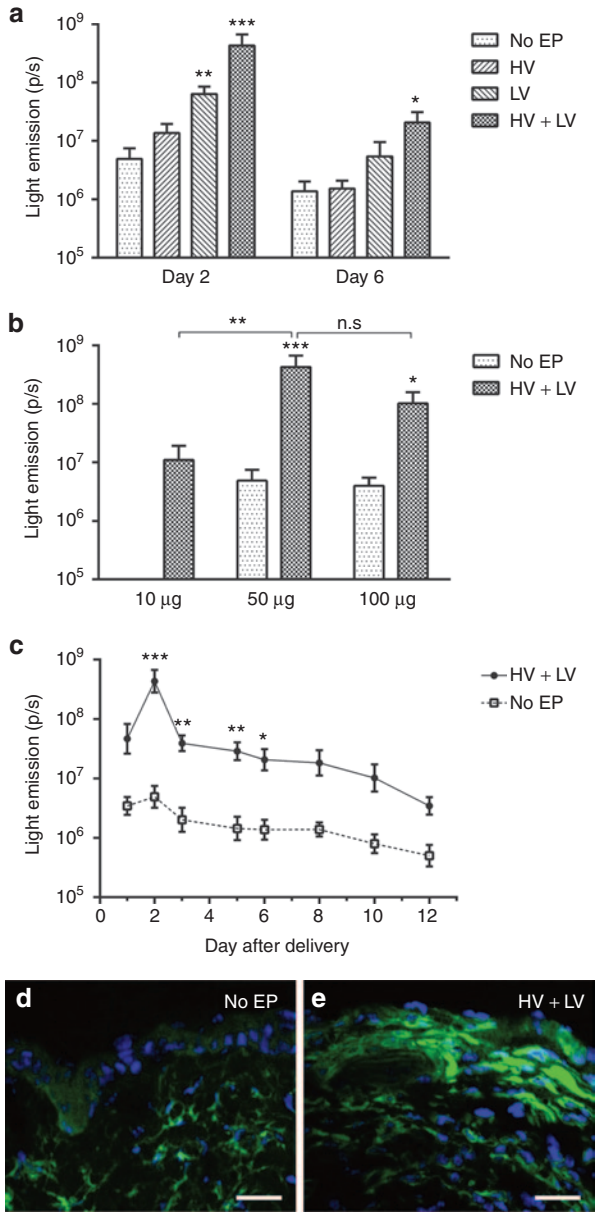

Figure 1 Optimization of DNA electroporation of cutaneous wounds. (**a**–**c**) *In vivo* luciferase imaging after DNA delivery. (**a**) Comparison of luciferase expression 2 and 6 days after intradermal injection of 50 µg of plasmid followed by (i) no electroporation (no EP), (ii) six 1,800 V/cm 100 µs high-voltage pulses with 125 µs pause (HV), (iii) ten 400 V/cm 20 ms low-voltage pulses with 125 µs pause (LV), and (iv) one 700 V/cm 100 µs and 200 V/cm 400 ms electric pulses (HV+LV). (**b**) Influence of the plasmid dose on luciferase expression after no EP or HV+LV. (**c**) Kinetics of luciferase expression over 12 days after no EP or HV+LV. Graphs represent the mean values (±SEM), $n = 5$. Statistical analysis: one-way ANOVA and Tukey post-test (n.s., not significant; $^*P < 0.05$, $^{**}P < 0.01$, $^{***}P < 0.001$). (**d**,**e**) Detection of GFP transcript. Five-micrometer thick cryosections of intact wound edges 2 days after injection of 50 µg of pGFP followed by (**d**) no EP or (**e**) HV+LV. Bar = 30 µm.

day 2, stayed significantly high over 6 days, and appeared to be elevated for at least 12 days (**Figure 1c**). Enhanced gene delivery by HV+LV DNA electroporation was confirmed by fluorescence microscopy using a green fluorescent protein (GFP) reporter plasmid (pGFP). Gene expression after intradermal injection of naked DNA plasmids was mainly located in the dermis of the skin without expression in the epidermis (**Figure 1d**). In contrast, electroporation using HV+LV electric pulses (**Figure 1e**) resulted in stronger gene expression that appeared predominantly in keratinocytes of the epidermis.

Electroporation of phCAP-18/LL-37 promoted wound healing in nondiabetic mice

Electroporation of plasmid pQE-hCAP-18/LL-37 (phCAP-18/LL-37) that encodes the propeptide hCAP-18 led to the expression of LL-37 peptide by keratinocytes at the intact wound edges. This

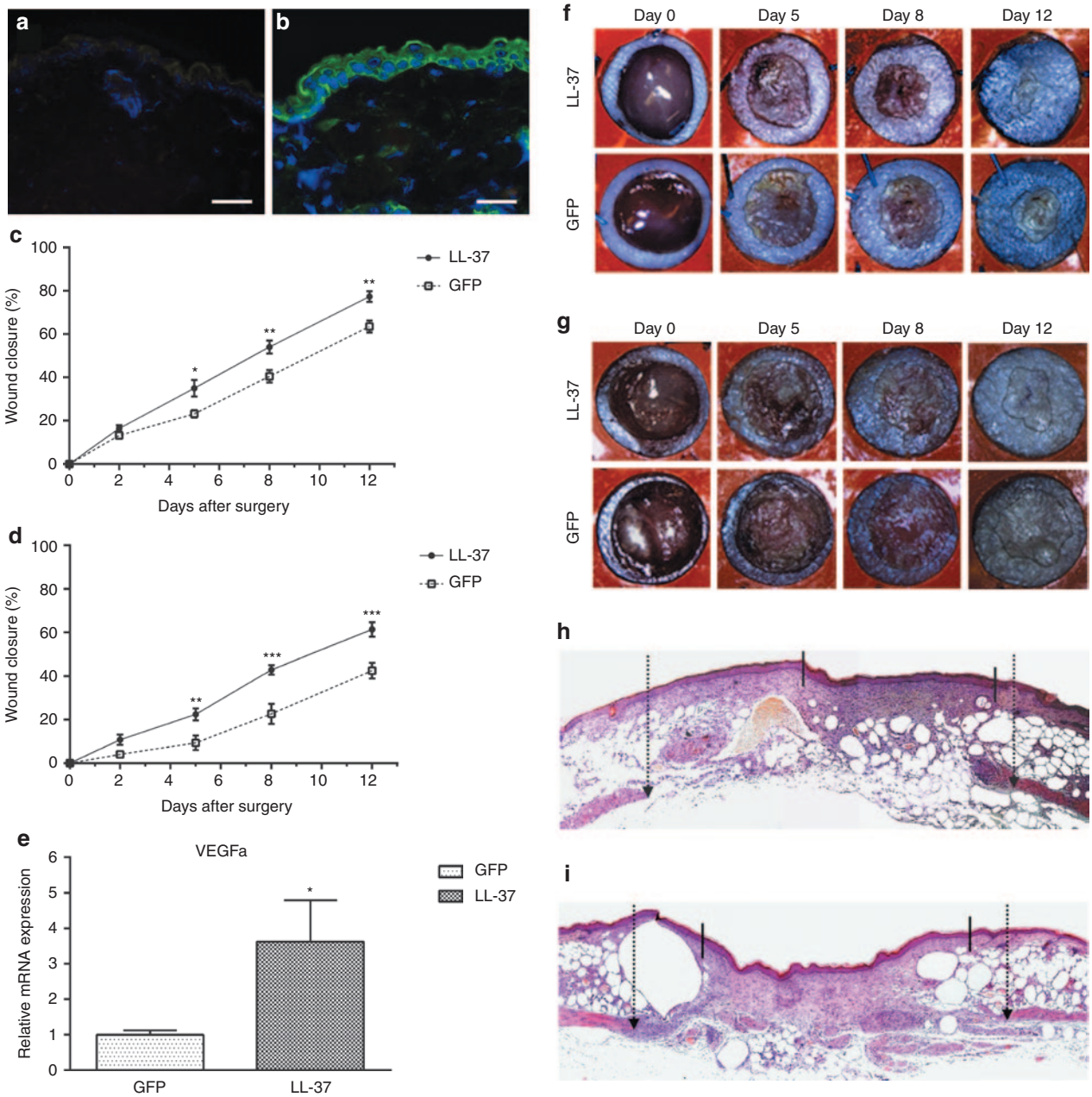

Figure 2 Electroporation of phCAP-18/LL-37 in wounds of C57BL/6 and db/db mice. (**a**,**b**) Detection of LL-37 transcript. 5 µm thick cryosections of intact wound edges 2 days after injection of 50 µg of phCAP-18/LL-37 followed by HV+LV. Immunohistochemistry using (**a**) anti-IgG control or (**b**) anti-LL-37. Bar = 30 µm. Follow-up of wound healing on splint model in (**c**,**f**) nondiabetic and (**d**,**g**) diabetic mice. Graphs represent the mean values (±SEM), $n = 5$ for C57BL/6 and $n = 6$ for db/db mice. Statistical analysis: two-way ANOVA and Bonferroni post-test (*$P < 0.05$, **$P < 0.01$, ***$P < 0.001$). (**e**) RT-PCR analysis of VEGFa mRNA expression 12 days after electroporation of diabetic mice with pGFP or phCAP-18/LL-37. Graph represents the mean values (±SEM) normalized to 18S rRNA, $n = 6$. Statistical analysis: *t*-test (*$P < 0.05$). (**h**,**i**) Follow-up of wound healing on wound histology stained with hematoxylin and eosin. Arrows indicate wounded panniculus carnosus by 4 mm punch biopsy, and bars demonstrate the wound edges of db/db mice 12 days after electroporation of (**h**) phCAP-18/LL-37 or (**i**) pGFP.

cutaneous overexpression was demonstrated after immunostaining with anti-LL-37 antibodies (**Figure 2a,b**). Electroporation of phCAP-18/LL-37 led to significantly earlier wound closure beginning on day 5 with 35 ± 9% closure versus 23 ± 4% for the GFP control wounds ($P < 0.05$, ANOVA). Wound healing was significantly improved from day 8 to day 12, showing on average 54 ± 7% and 77 ± 6% wound closure for LL-37 treatment versus 40 ± 7% and 63 ± 6% for GFP control wounds, ($P < 0.01$, ANOVA) (**Figure 2c,f**).

Electroporation of phCAP-18/LL-37 restored delayed diabetic wound healing

Electroporation of phCAP-18/LL-37 was further analyzed in leptin-receptor knock-out db/db mice, as a diabetic model for delayed wound healing. Blood glucose level measurements displayed an average of 272 ± 54 g/dl (mean ± SEM), confirming diabetes. Skin-targeted electroporation of phCAP-18/LL-37 promoted the reepithelialization of diabetic wounds. Digital analysis of the wound size demonstrated improved wound closure, evidenced from day 5 after electroporation for phCAP-18/LL-37 with 23 ± 7% versus 9 ± 8% for pGFP controls ($P < 0.01$, ANOVA). On day 8, wound sizes were reduced by 43 ± 5% versus 23 ± 11% for controls ($P < 0.001$, ANOVA). Finally, wound closure of LL-37 treated animals revealed 61 ± 8% versus 43 ± 9% in the control group ($P < 0.001$, ANOVA) (**Figure 2d,g**). Subsequent histological analysis confirmed more efficient wound healing in LL-37 treated diabetic wounds (**Figure 2h,i**). Electroporation of phCAP-18/LL-37 led to advanced approximation of the wound edges and the treated wounds were at a later state of reepithelialization, while pGFP control wounds displayed a larger distance between the wound borders. Reverse transcription polymerase chain reaction (RT-PCR) analysis demonstrated a significant induction of VEGFa in wounds ($P < 0.05$, *t*-test), 12 days after electotroporation of phCAP-18/LL-37 (**Figure 2e**).

Electroporation of phCAP-18/LL-37 upregulated IL-6 and the effect of hCAP-18/LL-37 was IL-6 dependent

RT-PCR analysis of acute nondiabetic and diabetic wounds 12 days after wounding revealed significant induction of IL-6 transcription in both nondiabetic and diabetic wounds after phCAP-18/LL-37 electroporation ($P < 0.01$, $P < 0.05$, *t*-test), (**Figure 3a**). To investigate the role of IL-6 on wounds treated by phCAP-18/LL-37, we performed *in vitro* wound migration assays with or without the addition of IL-6 blocking antibodies to LL-37–stimulated human HaCaT cells. A concentration of 0.5 µg/ml of LL-37 was able to stimulate cell migration ($P < 0.05$, *t*-test), (**Figure 3b**). Interestingly, LL-37 peptide-induced cell migration was reduced in the presence of anti-IL-6 antibody (**Figure 3b,c**). To determine the effect of LL-37 peptide with or without addition of the IL-6 blocking antibody on the proliferation of human HaCaT cells, a colorimetric cell proliferation BrdU (5-bromo-2′-deoxyuridine)-ELISA was used. No influence of either LL-37 or the addition of the IL-6 blocking antibody on the proliferation rate of human HaCaT cells was observed (**Figure 3d**). To confirm *in vivo* the role of IL-6 in the wound healing activity of phCAP-18/LL-37, wounds of nondiabetic mice depleted in IL-6 were treated by electroporation of either phCAP-18/LL-37 or pGFP control while mice. The anti-IL-6 treatment completely suppressed the wound healing activity of phCAP-18/LL-37 which became similar to pGFP control (**Figure 3e**).

Angiogenesis and reperfusion after induction of hindlimb ischemia were enhanced by intradermal electroporation of phCAP-18/LL-37

Next, we determined the effect of skin-targeted electroporation of phCAP-18/LL-37 in a previously described ischemic hindlimb model in mice,[29–31] using laser doppler imaging which allows quantification of perfusion. In order to treat the entire ischemic area, we doubled the dose of plasmid and we intradermally injected two sites each with 50 µg. Intradermal electroporation of phCAP-18/LL-37 enhanced blood perfusion in the ischemic hindlimb, suggesting an accelerated sprouting of new and more functional blood vessels[29] (**Figure 4a,b**). One week after surgery and cutaneous *in vivo* electroporation of phCAP-18/LL-37, more than 75 ± 11% reperfusion was achieved compared to 45 ± 11% with the pGFP control treatment ($P < 0.001$ ANOVA). pGFP-treated ischemic limbs still showed diminished perfusion, whereas electroporation of phCAP-18/LL-37 led to significant reperfusion of the ischemic gap between the proximal and distal resection points of the femoral vessels. The blood flow was increased by a factor of two and a 85 ± 7% recovery was obtained with intradermal electroporation of phCAP-18/LL-37 into the skin at day 12 after surgery, whereas the perfusion in the pGFP controls remained significantly reduced ($P < 0.001$ ANOVA).

Intradermal electroporation of phCAP-18/LL-37 protected against muscular atrophy in ischemic hindlimb

Mice were sacrificed 12 days after surgery and treatment in order to assess the muscular atrophy induced by hindlimb ischemia. The percentage of muscle atrophy, calculated by comparing ischemic gastrocnemius to the respective contralateral muscle, was 12 ± 5% for control mice treated by electroporation of pGFP and was significantly reduced to 4 ± 8% after phCAP-18/LL-37 electroporation (**Figure 4f**). Histology of the muscle fibers confirmed the protective effect of phCAP-18/LL-37 treatment against muscular atrophy (**Figure 4c–e**), in agreement with the drastic increase of phCAP-18/LL-37 induced blood perfusion.

Skin-targeted *in vivo* electroporation of phCAP-18/LL-37 stimulated the transcription of angiogenic cytokines and receptors in ischemic hindlimb muscles

Gastrocnemius muscle samples demonstrated a significant 2.5 to 3-fold induction of the transcription of angiogenic cytokines VEGFa and SDF-1a ($P < 0.05$, *t*-test), 12 days after the induction of ischemia and cutaneous electotroporation of phCAP-18/LL-37 (**Figure 4g,h**). These elevated cytokines were associated with a significant increase in the transcription of their receptors VEGFR-1 and CXCR-4 ($P < 0.05$, *t*-test) (**Figure 4i,j**). It has been suggested that quantitation of receptors for angiogenic cytokines by RT-PCR could reflect the presence of mobilized circulating angiogenic cells which characteristically express these receptors.[32,33]

DISCUSSION

We have previously described that transient cutaneous adenoviral delivery of hCAP-18/LL-37 combat wound infection in an infected rat burn model showed superiority to topical peptide treatment.[15] As our subsequent attempts at topical LL-37 peptide

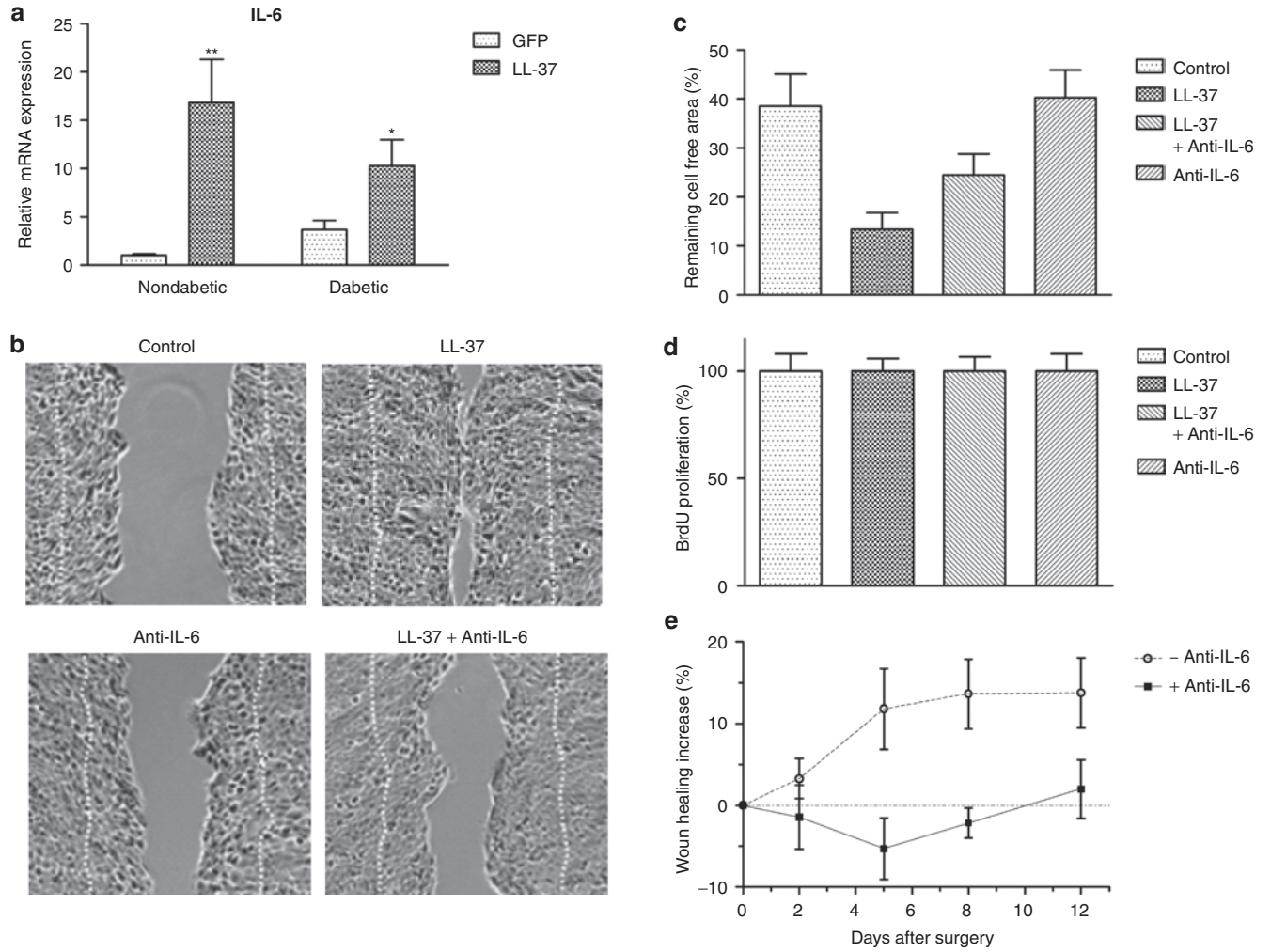

Figure 3 Role of IL-6 on keratinocyte migration and wound healing. (**a**) RT-PCR analysis of IL-6 mRNA expression after DNA electroporation of pGFP or phCAP-18/LL-37, normalized to 18S rRNA. Graph represents the mean values (±SEM), $n = 5$ for nondiabetic and $n = 6$ for diabetic mice. Statistical analysis: *t*-test (*$P < 0.05$, **$P < 0.01$). (**b**,**c**) *In vitro* wound migration and (**d**) BrdU proliferation assay. White dotted lines display the cell free area at day 0 after removal of silicone inserts. Human HaCaT cells were incubated for 24 hours in (i) 200 µg/ml anti-rabbit IgG as control, (ii) 0.5 µg/ml LL-37 peptide and 200 µg/ml anti-rabbit IgG, (iii) 0.5 µg/ml LL-37 peptide and 200 µg/ml anti-IL-6 or (iv) 200 µg/ml anti-IL-6. Graphs represent the mean values (±SEM), $n = 3$. Statistical analysis: one-way ANOVA and Tukey post-test (*$P < 0.05$). (**e**) Wound healing activity after DNA electroporation in C57BL/6 mice treated ($n = 7$) or not ($n = 5$) with anti-IL-6 mAb. Graph represents the mean value (±SEM) of the difference observed between phCAP-18/LL-37 and pGFP treatments. Statistical analysis: two-way ANOVA (*P* value: 0.0002).

treatment failed to promote consistent wound healing in murine models,[12] we hypothesized that skin-targeted electroporation of a plasmid encoding this host defense peptide would promote the healing of nondiabetic and diabetic wounds. We demonstrated here that the noninvasive electroporation of the wound edges was a convenient nonviral alternative for the direct treatment of wounds using a plasmid encoding hCAP-18 to overexpress LL-37.

First, we showed that gene expression in the wound area was higher and lasted significantly longer after electroporation with combined HV+LV pulses as compared to previously reported protocols involving administration of a series of pulses with the same field strength[27,28] (**Figure 1a**). In agreement with previous reports,[34,35] gene expression after intradermal injection of naked pGFP was mainly located in the dermis of the skin without expression in the epidermis (**Figure 2a**) whereas electroporation of pGFP induced strong expression predominantly in keratinocytes of the epidermis (**Figure 2b**). As keratinocytes adjacent to the wound bed are at the origin of reepithelialization,[36] we targeted the wound edges for promoting healing. Muscle contractions at the time of pulse application and local pain are reported adverse effects of electroporation.[37] Therefore, electrodes were designed to reduce potential pain during the application of a current.[38,39] Another approach to further reduce potential pain is to reduce the number of pulses: the use of high- and low-voltage pulse combinations have been discussed intensively, with the conclusion that the administration in two different steps provides permeabilization and electrophoresis to drive the DNA plasmid into the target cells *in vivo*.[40,41] By targeting the skin, this combination of pulses has been shown to significantly increase gene expression.[24,25,40] Using this optimized delivery method, we transfected the epidermal keratinocytes of the intact wound edges with phCAP-18/LL-37 as demonstrated by LL-37 immunohistochemistry (**Figure 2b**). Moreover, skin electroporation of phCAP-18/LL-37 was able to significantly improve wound closure in both nondiabetic

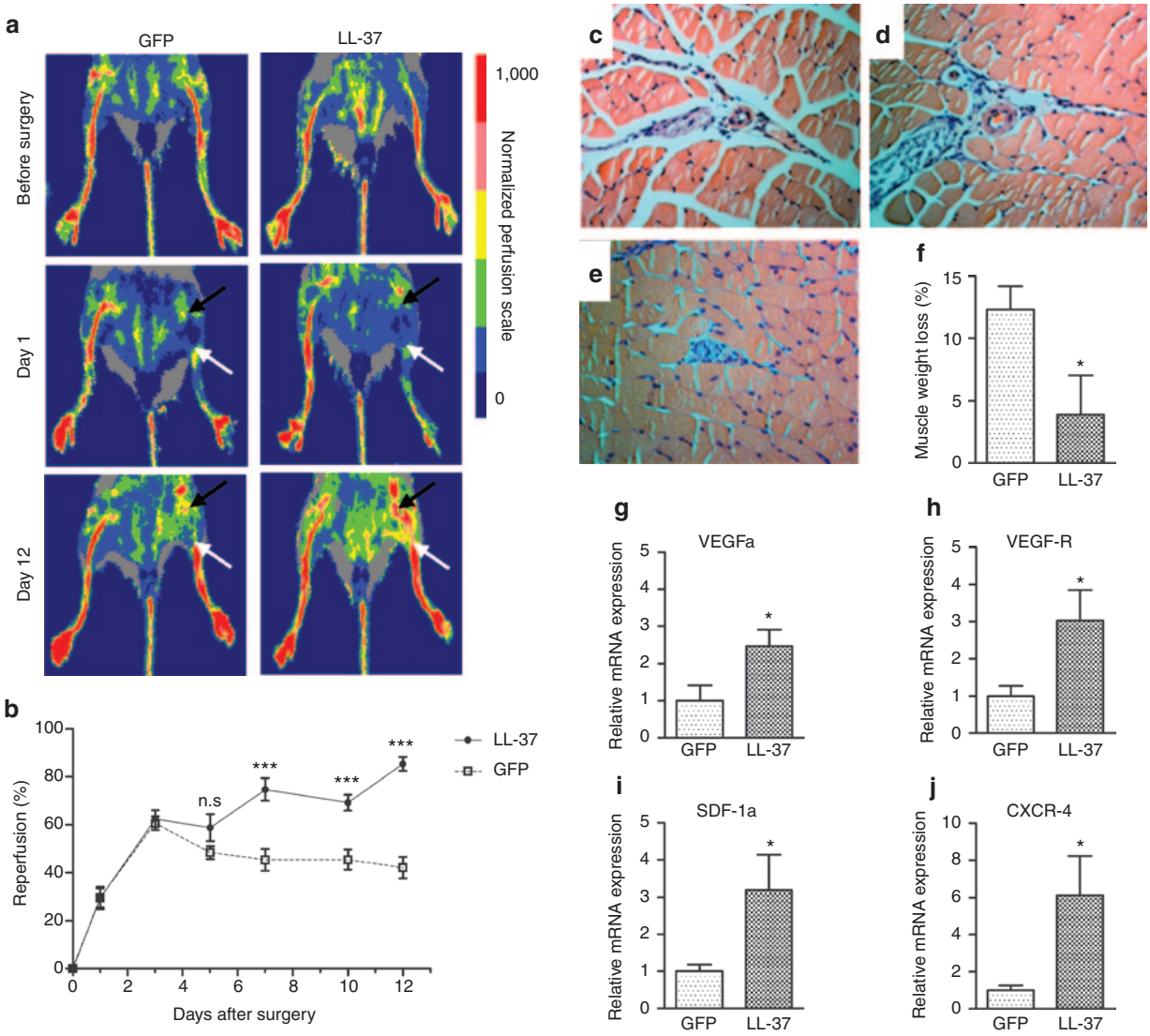

Figure 4 Blood perfusion, molecular atrophy, and expression of angiogenic cytokines and receptors after electroporation of phCAP-18/LL-37 in ischemic hindlimb model. (**a**,**b**) Follow-up of perfusion by laser Doppler imaging. Skin-targeted electroporation was performed at day 0 after surgery. Black arrows demonstrate the proximal and white arrows show the distal resection height of the femoral vessels. Graphs represent the mean values (±SEM), $n = 6$. Statistical analysis: two-way ANOVA and Bonferroni post-test (n.s., not significant; ***$P < 0.001$). Hematoxylin and eosin stained transverse muscle sections 12 days after cutaneous electroporation using (**c**) pGFP or (**d**) phCAP-18/LL-37 as compared to (**e**) healthy gastrocnemius muscle. (**f**) Muscle weight loss at day 12 after induction of ischemia and treatment. Graph represents the mean values (±SEM), $n = 6$. Statistical analysis: t-test (*$P < 0.05$). RT-PCR analysis of (**g**) VEGFa, (**h**) VEGF-R, (**i**) SDF-1a, and (**j**) CXCR-4 mRNA expression 12 days after electroporation of pGFP or phCAP-18/LL-37. Graphs represent the mean values (±SEM) normalized to 18S rRNA, $n = 6$. Statistical analysis: *t*-test (*$P < 0.05$).

(**Figure 2c**,**f**) and diabetic mice models (**Figure 2d**,**g**), confirming the hypothesis that skin-targeted electroporation induces an efficient nonviral delivery of host defense peptide in wounds.

Further, our study provided additional insights into an understanding of LL-37 induced wound healing by demonstrating the essential involvement of IL-6, a pleiotropic cytokine that can influence growth and differentiation of various cells types. It has been previously demonstrated that IL-6-deficient mice display a dramatic delay in wound healing.[42] Epidermal keratinocytes have been identified as the main source of IL-6 production in the skin[43] and several host defense peptides including LL-37 have been shown to stimulate IL-6 expression.[44] Here, we observed a significant increase in IL-6 transcription after electroporation of phCAP-18/LL-37 (**Figure 3a**). To shed light onto the influence of IL-6 for wound repair after overexpression of LL-37, we performed *in vitro* wound migration assays using human HaCaT cells. LL-37 stimulated cell migration without directly affecting cell proliferation, supporting previous results obtained using adenovirus-transfected HaCaT cells overexpressing LL-37.[45] Consistent with a major role for IL-6, the LL-37 peptide-induced cell migration was abolished in the presence of an IL-6 blocking antibody (**Figure 3b**,**c**). We also demonstrated that the wound healing activity promoted by electroporation of phCAP-18/LL-37 was suppressed when mice were concomitantly treated by IL-6 neutralizing antibody (**Figure 3e**). These *in vitro* and *in vivo* data thus strongly suggest that LL-37 promoted wound healing by inducing IL-6 dependent keratinocyte migration.

In the past, cutaneous electroporation of FGF-2 has promoted increased perfusion and angiogenesis in a hindlimb ischemia model.[46] Here, we propose that electroporation of phCAP-18/LL-37 into the skin after induction of hindlimb ischemia promoted neovascularization and the induction of pro-angiogenic cytokine expression in the muscle (**Figure 4**). The involvement of VEGF in LL-37 activity was initially denied as it was shown that the addition of anti-VEGF did not inhibit LL-37 induced proliferation of endothelial cells *in vitro*.[47] However, it has been shown later that LL-37 was able to regulate the overexpression of VEGF in keratinocytes.[48] In our study, we provide further evidence that LL-37 indeed has an influence on the expression of angiogenic cytokine, as VEGFa is significantly upregulated after electroporation of phCAP-18/LL-37 (**Figure 2e**, **4g**). It suggests that LL-37 induced VEGF expression after skin-targeted electroporation may contribute to the angiogenic effect of LL-37 *in vivo*. In addition, we observed reduced muscle atrophy when the ischemic limbs were treated by phCAP-18/LL-37 electroporation (**Figure 4f**).

The skin is an attractive target for drug delivery and local gene therapy, both in regard of its accessibility and behavior as immunocompetent organ. By delivering plasmid to wounds using electroporation, we have shown promising results that pave the way for potential clinical applications. As skin-targeted electroporation of LL-37 reduces ischemic injury its application in the clinical setting could help reducing surgical flap loss. Patients with peripheral artery disease could benefit from the revascularization potency of this new treatment. As LL-37 has displayed antimicrobial activity in preclinical studies, electroporation of LL-37 could greatly contribute to the treatment of wound infection and help restoring the underexpression of LL-37 in diabetic wounds.[11] Whereas our previous attempt of topical application of LL-37 failed to improve diabetic delayed wound healing,[12] local transient gene therapy using a plasmid encoding hCAP-18/LL-37 restored the healing of diabetic wounds.

In conclusion, we introduced a novel nonviral gene therapeutic technique to treat nondiabetic and wounds and to promote angiogenesis with LL-37. Moreover, we uncovered an IL-6 dependency for LL-37 induced wound healing *in vitro* and *in vivo*. More studies will be needed to further evaluate the clinical applicability of *in vivo* phCAP-18/LL-37 electroporation.

MATERIALS AND METHODS

Plasmids. Luciferase and green fluorescent protein genes originate from the pcDNA3.1-Luc (Invitrogen, Darmstadt, Germany) and the pEGFP-N1 (Clontech, Palo Alto, CA), respectively. The gene encoding human hCAP-18/LL-37 peptide originates from Ad5-hCAP-18 virus,[15] which was kindly provided by The Vector Core (Gene Therapy Program, Division of Medical Genetics, Department of Medicine, University of Pennsylvania). DNA cloning was performed using pQE-TriSystem plasmid vector (Qiagen, Hilden, Germany) according to the manufacturer's protocol. Briefly, the individual PCR products were gel purified and digested with BamHI and NotI (Luciferase), EcoRI and HindIII (GFP), and BamHI and HindIII (hCAP-18/LL-37). Inserts were then ligated with the pQE-TriSystem expression vector by T4 DNA ligase, transformed into *E. coli* XL-1-blue and selected on ampicillin containing LB agar plates. Plasmid purifications were carried out with endotoxin-free plasmid gigaprep (Qiagen) according to manufacturer's protocol and dissolved in sterile phosphate-buffered saline (PBS). The correct identity of each construct was confirmed by sequencing (GENterprise Genomics, Mainz, Germany).

Animals. Seven-week-old C57BL/6 mice (Janvier, Le Genest St Isle, France) were used for the luciferase protein expression assay and for the nondiabetic wound healing study. For the study of diabetic wound healing, 7-week-old leptin-receptor deficient db/db mice (Charles River, L'Arbresle, France) were used. Animals were anaesthetized using a mixture of ketamine (Anesketin, Eurovet, Heusden-Zolder, Belgium) and xylazine (Sigma, Bornem, Belgium) or by isoflurane inhalation. All experimental protocols with mice were approved by the Ethical Committee for Animal Care and Use of the Faculty of Medicine of the Université catholique de Louvain, Brussels, Belgium.

Electroporation of wounded skin. The dorsal surface was shaved 1 day prior to the experiments with depilatory cream (Veet for sensitive skin, Belgium), in order to thoroughly remove all hair. At the day of wounding, the dorsum of each anesthetized animal was disinfected with polyvidone iode. Two to four full-thickness wounds, one to two on each side of the midline, were created using a 4 mm punch biopsy. Plasmids diluted in sterile PBS to a total volume of 80 µl were intradermally injected in four quadrants around each wound. Each wound and the surrounded skin were then caught in between a 10 mm width and 2 mm spaced plate-electrode, and the electroporation was performed by a Cliniporator system (IGEA, Carpi, Italy). Three types of pulses were applied: (i) one 700 V/cm 100 µs and one 200 V/cm 400 ms electric pulses, without pause in between (HV+LV[24,25]), (ii) ten 400 V/cm 20 ms low-voltage pulses with 125 µs pauses between each pulse (LV[28]), or (iii) six 1,800 V/cm 100 µs high-voltage pulses with 125 µs pauses (HV[27]). For all experiments, conductive gel was applied to ensure electrical contact with the skin (EKO-GEL, ultrasound transmission gel, Egna, Italy).

In vivo *luciferase-Imaging.* Injection of a single dose of luciferin (150 mg/kg, ip, Promega, Leiden, Netherlands) at different time points after electroporation of pQE-Luciferase allowed *in vivo* detection of bioluminescence on an IVIS50 imaging system (Xenogen, Hopkinton, MA), as previously described.[49]

Immunostaining. Biopsy specimens were taken 2 days after electroporation of pGFP and phCAP-18/LL-37, frozen in liquid nitrogen-cooled isopentane and cut into five micrometer-thick cryosections. Sections of pGFP-treated wounds were rinsed with PBS and counterstained with the nuclear stain DAPI. Sections of hCAP-18/LL-37 wounds were immunostained with goat anti-rabbit-LL-37 antibody, kindly provided by Prof. Gallo (Division of Dermatology, Department of Medicine, University of California, San Diego, CA). The slides were incubated overnight with anti-LL-37 at 4 °C, then rinsed with PBS and incubated with biotinylated anti-goat antibody at room temperature. After the washing procedure, sections were incubated in streptavidin Alexa Fluor488. The slides were rinsed again and DAPI counterstaining was performed. Finally, the slides were covered with fluorescent mounting medium (Dako, Hamburg, Germany) and images were taken by using an Axioskop 2 plus microscope (Zeiss, Jena, Germany) connected to an AxioCam HRC camera (Zeiss).

Splint model for wound healing. To guaranty better reproducibility of the results by reducing wound contraction, wounds were fixed with a silicone splint. Donut-shaped splints with an outer diameter of 12 mm and an inner diameter of 6 mm were cut from a 0.5-mm thick silicone sheet (Grace Bio-Laboratories, Bend, OR). An immediate-bonding adhesive (Hollister, Libertyville, IL) was applied to fix the splint centrally to the wound, followed by 4-0 interrupted nylon sutures (Ethicon, Somerville, NJ). Wounds were covered by Jelonet paraffin gauze (Smith & Nephew, Hamburg, Germany) and Tegaderm as a transparent occlusive wound dressing (Tegaderm, 3M, Neuss, Germany), and changed every 2–3 days. The wound areas were digitally captured on days 0, 2, 5, 8, and 12 using a Leica IC80 HD stereo microscope with Leica LAS EZ V 1.8.0 Software (Leica, Heerbrugg, Switzerland). The wound size was evaluated using ImageJ 1.45s Software (National Institutes of Health,

Bethesda, MD) and calculated as the ratio of the wound borders to the inner 6 mm silicone ring. Results are expressed as the percentage of wound coverage compared to day 0 after surgery. To investigate the role of IL-6 in the healing process, nondiabetic mice received a daily intraperitoneal injection of 250 µg (in 250 µl PBS) of neutralizing anti-mouse IL-6 mAb (BioXcell, West Lebanon, NH), for 7 days, starting the day of surgery and electroporation. This protocol was previously described to deplete mice in IL-6.[50]

Quantitative real-time RT-PCR analysis of wound samples. Mice were sacrificed 12 days after treatment and the wound samples were taken and weighed to ensure that they did not to exceed 50 mg. Tissues were stored at −80 °C in RNAlater until further processing. Isolation of total RNA was done using Trizol, following the manufacturer's instructions for isolation of total RNA. RNA was eluted in a final volume of 30 µl RNase-free water. The concentration of RNA was determined using the Eppendorf Biophotometer (Eppendorf, Hamburg, Germany). One microgram of total RNA was transcribed into cDNA using the SuperScript II First Strand Synthesis System for RT-PCR (Invitrogen, Karlsruhe, Germany), following the manufacturer's instructions and using random hexamer primers. Relative quantification of mRNA was performed using the SYBR Green I fluorescent dye (Light Cycler FastStart DNA Master SYBR Green I, Roche Applied Science, Mannheim, Germany) and a Light Cycler 1.0 (Roche). The PCR reactions were performed with 2 µl of cDNA, 0.5 µmol/l of sense and antisense primers, 3 mmol/l $MgCl_2$ and 2 µl of FastStart SYBR Green reaction mix in a total volume of 20 µl. The cycling conditions were as follows: 95 °C for 10 minutes at a ramp speed of 20 °C/second, 50 cycles consisting of 94 ° C for 15 seconds at a ramp speed of 20 °C/second, a primer specific annealing temperature for 10 seconds at a ramp speed of 20 °C/second, 72 °C for 10 seconds at a ramp speed of 20 °C/second, followed by a melting point analysis: 95 °C for 0 second at a ramp speed of 20 °C/second, 65 °C for 15 seconds at a ramp speed of 20 °C/second, 95 °C for 0 second at a ramp speed of 0.1 °C/second, and finally a cooling phase: 40 °C for 30 seconds at a ramp speed of 20 °C/second. All primer pairs were validated to generate a single PCR product and mRNA concentrations were normalized to 18S rRNA in each sample and expressed as relative expression compared to controls. Primer sequences are as follows: 18S sense 5′–gaaactgcgaatggctcattaaa-3′ and 18S antisense 5′-cacagttatccaaggaggagg-3′; VEGFa[33] sense 5′-cttgttcagagcggagaaagc-3′, and antisense 5′-acatctgcaagtacgttcgtt-3′; IL-6 sense 5′-ccggagaggagacttcacag-3′ and antisense 5′-tccacgatttcccagagaac-3′.

Histology analysis of full-thickness wounds. Wound samples from each experiment were fixed in 4% buffered paraformaldehyde. Tissue samples were stained with hematoxylin/eosin and images taken with an AxioCam camera on an Axioplan microscope (Carl Zeiss GmbH, Oberkochen, Germany).

In vitro *wound migration assay.* HaCaT is a human epidermal keratinocyte-derived immortalized cell line. HaCaT cells (kindly supplied by Prof. Fusenig, University of Heidelberg, Germany), were cultured in Dulbecco's modified Eagle medium with 10% fetal bovine serum and 1% penicillin/streptomycin at 37 °C in humidified atmosphere at 5% CO_2. Culture medium was changed every second day. LL-37 was synthesized by The Nucleic Acid/Protein Synthesis Unit at University of British Columbia using solid phase FMOC-chemistry and purified to a purity >95% using reversed phase high-performance liquid chromatography. Peptide mass and lack of contaminating peptides were confirmed by mass spectrometry. HaCaT cells were seeded into 12-well plates, in each of the two compartments of Ibidi silicone chamber (12,500 cells in 80 µl/compartment) (Ibidi GmbH, Munich, Germany). After 24 hours the silicone chambers were carefully removed, cells were rinsed with PBS, and 1 ml culture medium was added, containing either anti-rabbit-IgG (200 µg/ml) as a control, anti-rabbit-IgG + LL-37 (0.5 µg/ml), anti-IL-6 (200 µg/ml) (Rockland, Gilbertsville, PA) or anti-IL-6 + LL-37 (0.5 µg/ml). Each experiment was performed in triplicate. Images were taken with an AxioCam camera on an Axioplan microscope (Carl Zeiss GmbH) directly after the addition of the indicated medium and 24 hours after their incubation. The wound size was evaluated using ImageJ 1.45s Software (National Institutes of Health) and the results are expressed in percent as ratio of the cell free area after 24 hours of incubation compared to the area before incubation.

BrdU proliferation assay. A colorimetric cell proliferation assay involving incorporation of BrdU (5-bromo-2′-deoxyuridine)-ELISA (Roche) was performed according to the manufacturer's protocol. HaCaTs were seeded in a 96-well microtiterplate (Omnilab, Bremen, Germany). After 24 hours, either anti-rabbit-IgG (200 µg/ml) as control, anti-rabbit-IgG + LL-37 (0.5 µg/ml), anti-IL-6 (200 µg/ml), or anti-IL-6 + LL-37 (0.5 µg/ml) were added. Each experiment was performed in triplicates. After additional incubation of 24 hours, anti-BrdU conjugated to peroxidase was added. Based on the incorporation of the thymidine analogue BrdU during DNA-synthesis, proliferation of HaCaT cells was indirectly quantified by using a microplate absorbance reader Sunrise (Tecan trading AG, Männedorf, Switzerland). KC4 software (BioTek 34 Instruments, Bad Friedrichshall, Germany) was used for the analysis.

Ischemic hindlimb model. The femoral artery and vein ligation and resection model was used as described previously.[29–31] The mice were anaesthetized as described above and both hindlimbs were shaved. After incision of the skin at the lateral thigh, mice underwent unilateral 10-mm–length resection of the proximal femoral artery and vein under a stereoscopic microscope. The femoral nerve was carefully preserved during the microsurgical procedure. After skin closure, 100 µg of phCAP-18/LL-37 or pGFP to a total volume of 80 µl PBS were intradermally injected above the resection area. The entire limb was then placed between a 10 mm width and 4 mm spaced plate-electrode and the electroporation was performed using a Cliniporator system (IGEA, Carpi, Italy) with a combination of one high-voltage (700 V/cm, 100 µs) and one low-voltage (200 V/cm, 400 ms) electric pulse. On the indicated days, anesthetized mice were placed on a heating pad (37 °C), and the perfusion of both the wounded and the contralateral healthy hindlimb was measured using a Laser Doppler Flowmeter (Moor Instruments, Axminster, UK). Blood perfusion of the ischemic area was quantified on the basis of colored pixel histograms and normalized to the perfusion of the healthy contralateral leg of the same animal. Results are expressed as percentage of reperfusion compared to day 0 after surgery.

Determination of muscular atrophy. Mice were sacrificed 12 days after femoral artery and vein dissection. For the assessment of skeletal muscle atrophy gastrocnemius muscles from the ischemic and healthy hindlimb were carefully microdissected from adjacent tissue and weighted. Muscle weight loss was calculated as weight ratio between the ischemic and the contralateral healthy muscle of each animal. For histological analysis tissue samples were sectioned perpendicularly to the main axis, and fixed in 4% buffered paraformaldehyde. Cross sections were stained with hematoxylin/eosin and images taken with an AxioCam camera on an Axioplan microscope (Carl Zeiss GmbH).

RT-PCR analysis of the muscle tissue of ischemic hindlimbs. Gastrocnemius muscles were sampled and processed as described above. Primer sequences for angiogenic cytokines and their receptors are as follows:[33] VEGFa sense 5′-cttgttcagagcggagaaagc-3′, and antisense 5′-acatctgcaagtacgttcgtt-3′; SDF-1a sense 5′-gagagccacatcgccagag-3′, and antisense 5′-tttcgggtcaatgcacacttg-3′; VEGFR-1 sense 5′-tggacccagatgaagttccc-3′, and antisense 5′-gcgatttgcctagtttcagtct -3′; CXCR-4 sense 5′-agcatgacggacaagtacc-3′, and antisense 5′-gatgatatggacagccttacac-3′.

Statistical analysis. Results are presented as means ± SEM. Differences in means between groups were analyzed for significance using Student's *t*-test or ANOVA as appropriate (GraphPad Prism Software, San Diego, CA).

ACKNOWLEDGMENTS

We thank Bernard Ucakar, Kevin Vanvarenberg, and Andrea Rittig for their excellent technical contribution to this work. This work was supported by grants from the Belgian Fonds National de la Recherche Scientifique (F.R.S.-FNRS), an Action de Recherche Concertée from the Communauté Française de Belgique and Belgian Federal Agency for Nuclear Control (AFCN-FANC, grant P.0. 4500020406) (to P.S.), and by the Fonds Spéciaux de la Recherche (FSR). M.C.L. is a scholar of the Friedrich-Naumann Foundation. K.K.C. is an early stage researcher (ESR) of FP7 Marie Curie NANODRUG network. R.E.W.H. holds a Canada Research Chair and is funded by a Canadian Institutes for Health Research grant. P.S. is a Research Associate and G.V. a Postdoctoral Researcher of the F.R.S.-FNRS. The authors declare are no conflict of interest.

REFERENCES

1. Vinh, DC and Embil, JM (2005). Rapidly progressive soft tissue infections. *Lancet Infect Dis* **5**: 501–513.
2. Rice, LB (2003). Do we really need new anti-infective drugs? *Curr Opin Pharmacol* **3**: 459–463.
3. Grundmann, H, Aires-de-Sousa, M, Boyce, J and Tiemersma, E (2006). Emergence and resurgence of meticillin-resistant Staphylococcus aureus as a public-health threat. *Lancet* **368**: 874–885.
4. Hancock, RE and Sahl, HG (2006). Antimicrobial and host-defense peptides as new anti-infective therapeutic strategies. *Nat Biotechnol* **24**: 1551–1557.
5. Sørensen, OE, Follin, P, Johnsen, AH, Calafat, J, Tjabringa, GS, Hiemstra, PS *et al.* (2001). Human cathelicidin, hCAP-18, is processed to the antimicrobial peptide LL-37 by extracellular cleavage with proteinase 3. *Blood* **97**: 3951–3959.
6. Steinstraesser, L, Koehler, T, Jacobsen, F, Daigeler, A, Goertz, O, Langer, S *et al.* (2008). Host defense peptides in wound healing. *Mol Med* **14**: 528–537.
7. Steinstraesser, L, Al-Benna, S, Kesting, M and Jacobsen, F (2009). Bioengineered human skin: working the bugs out. *Mol Ther* **17**: 405–408.
8. Heilborn, JD, Nilsson, MF, Kratz, G, Weber, G, Sørensen, O, Borregaard, N *et al.* (2003). The cathelicidin anti-microbial peptide LL-37 is involved in re-epithelialization of human skin wounds and is lacking in chronic ulcer epithelium. *J Invest Dermatol* **120**: 379–389.
9. Nizet, V, Ohtake, T, Lauth, X, Trowbridge, J, Rudisill, J, Dorschner, RA *et al.* (2001). Innate antimicrobial peptide protects the skin from invasive bacterial infection. *Nature* **414**: 454–457.
10. Dressel, S, Harder, J, Cordes, J, Wittersheim, M, Meyer-Hoffert, U, Sunderkötter, C *et al.* (2010). Differential expression of antimicrobial peptides in margins of chronic wounds. *Exp Dermatol* **19**: 628–632.
11. Rivas-Santiago, B, Trujillo, V, Montoya, A, Gonzalez-Curiel, I, Castañeda-Delgado, J, Cardenas, A *et al.* (2012). Expression of antimicrobial peptides in diabetic foot ulcer. *J Dermatol Sci* **65**: 19–26.
12. Steinstraesser, L, Hirsch, T, Schulte, M, Kueckelhaus, M, Jacobsen, F, Mersch, EA *et al.* (2012). Innate defense regulator peptide 1018 in wound healing and wound infection. *PLoS ONE* **7**: e39373.
13. Schmidtchen, A, Frick, IM, Andersson, E, Tapper, H and Björck, L (2002). Proteinases of common pathogenic bacteria degrade and inactivate the antibacterial peptide LL-37. *Mol Microbiol* **46**: 157–168.
14. Carretero, M, Del Río, M, García, M, Escámez, MJ, Mirones, I, Rivas, L *et al.* (2004). A cutaneous gene therapy approach to treat infection through keratinocyte-targeted overexpression of antimicrobial peptides. *FASEB J* **18**: 1931–1933.
15. Jacobsen, F, Mittler, D, Hirsch, T, Gerhards, A, Lehnhardt, M, Voss, B *et al.* (2005). Transient cutaneous adenoviral gene therapy with human host defense peptide hCAP-18/LL-37 is effective for the treatment of burn wound infections. *Gene Ther* **12**: 1494–1502.
16. Nikol, S (2007). Viral or non-viral angiogenesis gene transfer-New answers to old questions. *Cardiovasc Res* **73**: 443–445.
17. Thomas, CE, Ehrhardt, A and Kay, MA (2003). Progress and problems with the use of viral vectors for gene therapy. *Nat Rev Genet* **4**: 346–358.
18. Mäkinen, K, Manninen, H, Hedman, M, Matsi, P, Mussalo, H, Alhava, E *et al.* (2002). Increased vascularity detected by digital subtraction angiography after VEGF gene transfer to human lower limb artery: a randomized, placebo-controlled, double-blinded phase II study. *Mol Ther* **6**: 127–133.
19. Vogt, PM, Thompson, S, Andree, C, Liu, P, Breuing, K, Hatzis, D *et al.* (1994). Genetically modified keratinocytes transplanted to wounds reconstitute the epidermis. *Proc Natl Acad Sci USA* **91**: 9307–9311.
20. Zhang, Z, Slobodianski, A, Ito, WD, Arnold, A, Nehlsen, J, Weng, S *et al.* (2011). Enhanced collateral growth by double transplantation of gene-nucleofected fibroblasts in ischemic hindlimb of rats. *PLoS ONE* **6**: e19192.
21. Nauta, A, Seidel, C, Deveza, L, Montoro, D, Grova, M, Ko, SH *et al.* (2013). Adipose-derived stromal cells overexpressing vascular endothelial growth factor accelerate mouse excisional wound healing. *Mol Ther* **21**: 445–455.
22. Thomas-Virnig, CL, Centanni, JM, Johnston, CE, He, LK, Schlosser, SJ, Van Winkle, KF *et al.* (2009). Inhibition of multidrug-resistant Acinetobacter baumannii by nonviral expression of hCAP-18 in a bioengineered human skin tissue. *Mol Ther* **17**: 562–569.
23. Satkauskas, S, Bureau, MF, Puc, M, Mahfoudi, A, Scherman, D, Miklavcic, D *et al.* (2002). Mechanisms of *in vivo* DNA electrotransfer: respective contributions of cell electropermeabilization and DNA electrophoresis. *Mol Ther* **5**: 133–140.
24. Pavselj, N and Préat, V (2005). DNA electrotransfer into the skin using a combination of one high- and one low-voltage pulse. *J Control Release* **106**: 407–415.
25. Vandermeulen, G, Staes, E, Vanderhaeghen, ML, Bureau, MF, Scherman, D and Préat, V (2007). Optimisation of intradermal DNA electrotransfer for immunisation. *J Control Release* **124**: 81–87.
26. Lee, PY, Chesnoy, S and Huang, L (2004). Electroporatic delivery of TGF-beta1 gene works synergistically with electric therapy to enhance diabetic wound healing in db/db mice. *J Invest Dermatol* **123**: 791–798.
27. Marti, G, Ferguson, M, Wang, J, Byrnes, C, Dieb, R, Qaiser, R *et al.* (2004). Electroporative transfection with KGF-1 DNA improves wound healing in a diabetic mouse model. *Gene Ther* **11**: 1780–1785.
28. Liu, L, Marti, GP, Wei, X, Zhang, X, Zhang, H, Liu, YV *et al.* (2008). Age-dependent impairment of HIF-1alpha expression in diabetic mice: Correction with electroporation-facilitated gene therapy increases wound healing, angiogenesis, and circulating angiogenic cells. *J Cell Physiol* **217**: 319–327.
29. Porporato, PE, Payen, VL, De Saedeleer, CJ, Préat, V, Thissen, JP, Feron, O *et al.* (2012). Lactate stimulates angiogenesis and accelerates the healing of superficial and ischemic wounds in mice. *Angiogenesis* **15**: 581–592.
30. Couffinhal, T, Silver, M, Zheng, LP, Kearney, M, Witzenbichler, B and Isner, JM (1998). Mouse model of angiogenesis. *Am J Pathol* **152**: 1667–1679.
31. Sonveaux, P, Martinive, P, DeWever, J, Batova, Z, Daneau, G, Pelat, M *et al.* (2004). Caveolin-1 expression is critical for vascular endothelial growth factor-induced ischemic hindlimb collateralization and nitric oxide-mediated angiogenesis. *Circ Res* **95**: 154–161.
32. Bosch-Marce, M, Okuyama, H, Wesley, JB, Sarkar, K, Kimura, H, Liu, YV *et al.* (2007). Effects of aging and hypoxia-inducible factor-1 activity on angiogenic cell mobilization and recovery of perfusion after limb ischemia. *Circ Res* **101**: 1310–1318.
33. Botusan, IR, Sunkari, VG, Savu, O, Catrina, AI, Grünler, J, Lindberg, S *et al.* (2008). Stabilization of HIF-1alpha is critical to improve wound healing in diabetic mice. *Proc Natl Acad Sci USA* **105**: 19426–19431.
34. Chesnoy, S and Huang, L (2002). Enhanced cutaneous gene delivery following intradermal injection of naked DNA in a high ionic strength solution. *Mol Ther* **5**: 57–62.
35. Meuli, M, Liu, Y, Liggitt, D, Kashani-Sabet, M, Knauer, S, Meuli-Simmen, C *et al.* (2001). Efficient gene expression in skin wound sites following local plasmid injection. *J Invest Dermatol* **116**: 131–135.
36. Sivamani, RK, Garcia, MS and Isseroff, RR (2007). Wound re-epithelialization: modulating keratinocyte migration in wound healing. *Front Biosci* **12**: 2849–2868.
37. Miklavcic, D, Pucihar, G, Pavlovec, M, Ribaric, S, Mali, M, Macek-Lebar, A *et al.* (2005). The effect of high frequency electric pulses on muscle contractions and antitumor efficiency *in vivo* for a potential use in clinical electrochemotherapy. *Bioelectrochemistry* **65**: 121–128.
38. Ferraro, B, Heller, LC, Cruz, YL, Guo, S, Donate, A and Heller, R (2011). Evaluation of delivery conditions for cutaneous plasmid electrotransfer using a multielectrode array. *Gene Ther* **18**: 496–500.
39. Daugimont, L, Baron, N, Vandermeulen, G, Pavselj, N, Miklavcic, D, Jullien, MC *et al.* (2010). Hollow microneedle arrays for intradermal drug delivery and DNA electroporation. *J Membr Biol* **236**: 117–125.
40. Heller, LC, Jaroszeski, MJ, Coppola, D, McCray, AN, Hickey, J and Heller, R (2007). Optimization of cutaneous electrically mediated plasmid DNA delivery using novel electrode. *Gene Ther* **14**: 275–280.
41. André, FM, Gehl, J, Sersa, G, Préat, V, Hojman, P, Eriksen, J *et al.* (2008). Efficiency of high- and low-voltage pulse combinations for gene electrotransfer in muscle, liver, tumor, and skin. *Hum Gene Ther* **19**: 1261–1271.
42. Gallucci, RM, Sloan, DK, Heck, JM, Murray, AR and O'Dell, SJ (2004). Interleukin 6 indirectly induces keratinocyte migration. *J Invest Dermatol* **122**: 764–772.
43. Sehgal, PB (1990). Interleukin-6: molecular pathophysiology. *J Invest Dermatol* **94**(6 Suppl): 2S–6S.
44. Niyonsaba, F, Ushio, H, Nakano, N, Ng, W, Sayama, K, Hashimoto, K *et al.* (2007). Antimicrobial peptides human beta-defensins stimulate epidermal keratinocyte migration, proliferation and production of proinflammatory cytokines and chemokines. *J Invest Dermatol* **127**: 594–604.
45. Carretero, M, Escámez, MJ, García, M, Duarte, B, Holguín, A, Retamosa, L *et al.* (2008). *In vitro* and *in vivo* wound healing-promoting activities of human cathelicidin LL-37. *J Invest Dermatol* **128**: 223–236.
46. Ferraro, B, Cruz, YL, Baldwin, M, Coppola, D and Heller, R (2010). Increased perfusion and angiogenesis in a hindlimb ischemia model with plasmid FGF-2 delivered by noninvasive electroporation. *Gene Ther* **17**: 763–769.
47. Koczulla, R, von Degenfeld, G, Kupatt, C, Krötz, F, Zahler, S, Gloe, T *et al.* (2003). An angiogenic role for the human peptide antibiotic LL-37/hCAP-18. *J Clin Invest* **111**: 1665–1672.
48. Rodríguez-Martínez, S, Cancino-Diaz, JC, Vargas-Zuñiga, LM and Cancino-Diaz, ME (2008). LL-37 regulates the overexpression of vascular endothelial growth factor (VEGF) and c-IAP-2 in human keratinocytes. *Int J Dermatol* **47**: 457–462.
49. Marie, C, Vandermeulen, G, Quiviger, M, Richard, M, Préat, V and Scherman, D (2010). pFARs, plasmids free of antibiotic resistance markers, display high-level transgene expression in muscle, skin and tumour cells. *J Gene Med* **12**: 323–332.
50. Lin, ZQ, Kondo, T, Ishida, Y, Takayasu, T and Mukaida, N (2003). Essential involvement of IL-6 in the skin wound-healing process as evidenced by delayed wound healing in IL-6-deficient mice. *J Leukoc Biol* **73**: 713–721.